Quantitative modeling of laser speckle imaging

Pavel Zakharov and Andreas Völker

Department of Physics, University of Fribourg, 1700 Fribourg, Switzerland

Alfred Buck and Bruno Weber

Division of Nuclear Medicine, University Hospital Zurich, 8091 Zurich, Switzerland

Frank Scheffold

Department of Physics, University of Fribourg, 1700 Fribourg, Switzerland

We have analyzed the image formation and dynamic properties in laser speckle imaging (LSI) both experimentally and with Monte-Carlo simulation. We show for the case of a liquid inclusion that the spatial resolution and the signal itself are both significantly affected by scattering from the turbid environment. Multiple scattering leads to blurring of the dynamic inhomogeneity as detected by LSI. The presence of a non-fluctuating component of scattered light results in the significant increase in the measured image contrast and complicates the estimation of the relaxation time. We present a refined processing scheme that allows a correct estimation of the relaxation time from LSI data.

Laser speckle imaging (LSI) is an efficient and simple method for full-field monitoring of dynamics in heterogeneous media.[1] It is widely used in biomedical imaging of blood flow[1–5] since it provides access to physiological processes *in vivo* with excellent temporal and spatial resolution.

In a more general context LSI can be considered a simplified version of the dynamic light scattering (DLS) approach, which analyzes the temporal intensity fluctuations of scattered laser light in order to derive the microscopic properties of the scatterers position and motion.[6,7] In LSI an image of dynamic heterogeneities is obtained by analysing the local speckle contrast K in the image plane. K is defined by the variance of the intensity fluctuations for a given integration time T:[8] $K^2(T) = \langle I^2\rangle/\langle I\rangle^2 - 1$. In the absence of scatterers motion the contrast takes a maximum value, while motion decreases the contrast. Therefore the value K can be used to construct an image of local dynamic properties.[1] However the quantitative interpretation of the LSI data is not straightforward. Multiple scattering of light can influence the apparent size of the object due to diffuse blurring. Access to the local dynamic properties, such as blood flow or Brownian motion, is complicated by the complex interplay between the measured contrast and the full fluctuation spectrum of scattered light. The latter is usually not accessible if technical simplicity of LSI is to be preserved.

In this letter we present a quantitative approach to analyze LSI images. We address the problem of spatial resolution and blurring due to multiple scattering via model experiments and Monte-Carlo simulations. Further we will demonstrate that previous attempts to relate quantitatively LSI images to the microscopic motion have been hampered by an incorrect data analysis.We present a refined processing scheme to access this information from a standard LSI experiment. The main new element of our analysis is to take into account the contribution of the non-fluctuating part of scattered intensity. We furthermore suggest a simple experimental procedure that allows to access this important quantity.

Model experiments have been carried out using a homogeneous block of solid Teflon and a home-made heterogeneous sample. This medical phantom mimics a liquid inclusion in solid tissue. It is obtained by milling a cylindrical hole of diameter $D = 3$ mm in a block of solid Teflon. A layer of variable thickness $0.1 - 2.1$ mm separates the cylindrical inclusion from the interface that is imaged. The void is filled with a dispersion of 710 nm polystyrene particles in water. The particle concentration is adjusted to match the optical properties of the liquid dispersion to the solid such that no static scattering differences could be detected anymore (volume fraction ca. 1.3%; scattering coefficient $\mu_s = 36$ mm^{-1}, mean free path $l^* \simeq 277$ μm and anisotropy factor $g \approx 0.9$). The imaging setup has been described in detail in Ref. 5. Briefly, the cylindric inclusion with flat base of 3 mm diameter oriented to the surface is imaged with a CCD camera (PCO Pixelfly, Germany, exposure time 130 ms) with a standard camera objective lens ($f = 50$ mm). The sample is illuminated with a diode laser (wavelength 785 nm, max. 50 mW). Two crossed polarizers, positioned before and after the sample, ensure that we detect only depolarized light back reflected from the sample. The incident beam is expanded by a slow-rotating ground glass in order to reduce statistical noise.[5] For each depth the contrast as a function of radial distance r from the inclusion center is determined (Fig. 1).

For the Monte-Carlo simulation we followed the photon packet approach of light propagation in a turbid

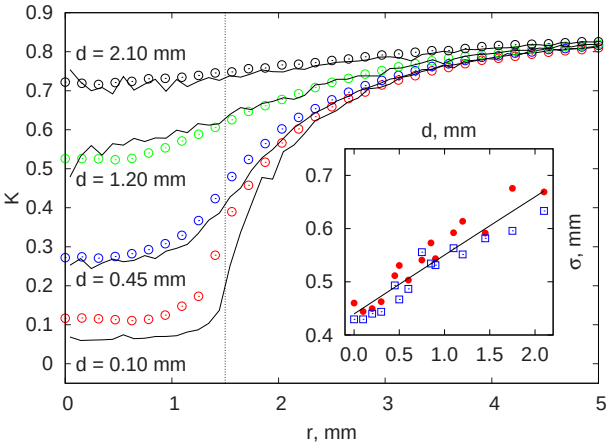

Fig. 1. Contrast K as a function of distance r from the center of the inclusion for different depths d. Lines - simulation results, Symbols - experimental results. Dotted line - inclusion boundary. Inset: Width of the liquid solid-boundary as a function of depth (● - simulation data, □ - experiment, line is a guide for the eye).

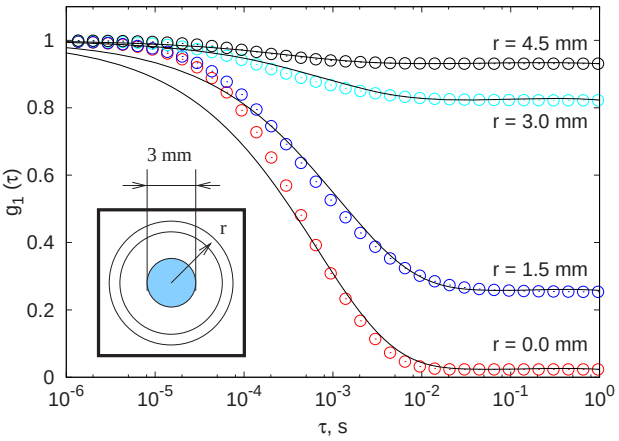

Fig. 2. Simulated correlation functions for the inclusion depth $d = 100\ \mu m$ (Symbols). Solid lines: Fits with DWS theory including a baseline; τ_0 values for the fits were obtained by the contrast K inversion (see Fig. 3).

medium.[9] The Henyey-Greenstein phase function was used based on an average scattering angle $\langle \cos\theta \rangle$.[9] The degree of polarization was assumed to decay exponentially.[10] The reflections and refractions on the boundaries were treated according to Fresnel formulas. Depolarized photon packets back-reflected from the sample where registered within a numerical aperture 0.17. The field auto-correlation function (ACF) $g_1(\tau)$ of the scattered light was determined as explained in Ref. 7.

In order to quantify the effect of image blurring caused by multiple scattering we determine the standard deviation σ of the contrast gradient dK/dr which is a measure of the *apparent* interfacial width. As shown in Fig. 1, starting from the smallest depths, the apparent width is increased. This increase is of the order of a few l^*, which is the relevant length scale for an incident photon to propagate laterally. The smearing increases linearily with depth until for large depths 2σ becomes of the order of the depth d, as expected for diffuse light propagation.[11] Our results show the importance of diffuse blurring in the image formation already for small and moderate depths and can thus provide important guidelines for experiments in biomedical imaging.[2,3]

A typical set of simulated correlation functions is presented in the Fig.2. If $g_1(\tau)$ is known, then the speckle contrast K of the time-integrated speckle fluctuations can be obtained via the following relation[12,13]

$$K^2(T) = \frac{\langle I^2 \rangle}{\langle I \rangle^2} - 1 = \frac{2}{T} \int_0^T \beta |g_1(\tau)|^2 \, (1 - \tau/T) \, d\tau, \quad (1)$$

where T is the integration time of the detector and $\beta \leq 1$ the coherence factor of the detection optics. Note that this equation differs from the traditionally used expression of Fercher and Briers.[1] As pointed out by Durian and coworkers[13] the expression of Fercher and Briers is incorrect and it is important to take into account *triangular averaging* of the correlation function via the factor $(1 - \tau/T)$.[12] As shown in Fig. 1 the resulting values of the contrast are found in quantitative agreement with the experimental data.

A comparison of Fig. 1 and Fig. 2 immediately reveals the main limitation of LSI. A single contrast value K is recorded in practice as compared to the complex correlation function characterizing the full spectrum of intensity fluctuations. To address this problem we first analyze the characteristic features of the correlation functions presented in Fig. 2. Overall the functions are well described by the usual stretched-exponential form derived for diffusing-wave spectroscopy (DWS) of a colloid suspension: $g_1(\tau) = \exp(-\gamma\sqrt{6\tau/\tau_0})$, where in our case the relaxation time $\tau_0 = 1/Dk_0^2$ characterizes Brownian motion (diffusion coefficient D) and $\gamma \simeq 2$ is a constant.[7] It is worthwhile to note that for the case of fluid flow the relaxation time τ_0 is inversely proportional to the characteristic velocity of the scatterers.[1,14]

The presence of a non-fluctuating static scattering part, however, leads to a non-zero baseline for the ACF. Since the relative amount of the static light scattering increases with the distance r from the center, the plateau of the ACF increases as well. It has been noted previously that a non-zero baseline significantly influences the resulting values of the contrast K.[1] Nevertheless it is rather common in the biomedical community to convert the obtained contrast values directly to relaxation times neglecting contributions of static scattering.[3,4,15]

If the detected light is composed of dynamic and static components: $E(\tau) = E_d(\tau) + E_s$ the field ACF is defined as following:[11]

$$g_1(\tau) = \langle E(\tau)E(0) \rangle / \langle E \rangle^2 = (1 - \rho) \, |g_{1\,\mathrm{d}}(\tau)| + \rho, \quad (2)$$

where $\rho = \langle I_s \rangle / (\langle I_d \rangle + \langle I_s \rangle)$ characterizes the static part of the detected light intensity and $g_{1\,\mathrm{d}}(\tau)$ is the field

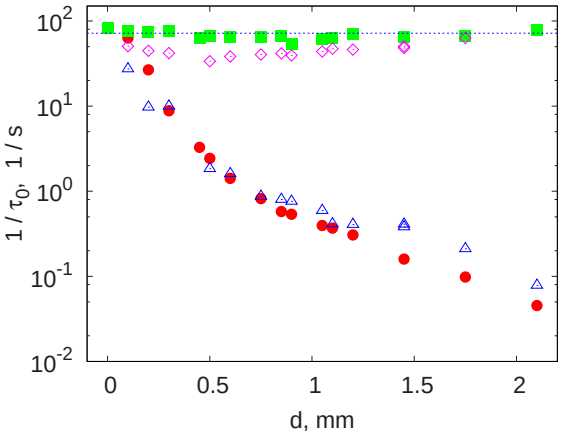

Fig. 3. Inverse of the relaxation time $1/\tau_0$ as a function of depth obtained by directly converting the contrast $K(r \approx 0)$ based on Eq.1 neglecting the static part: ● - simulation data, △ - experiment and using the correct procedure based on Eq. 3: ■ - simulation and ◊ - experiment. Horizontal dashed line - actual value of the relaxation time $1/\tau_0 \simeq 72s^{-1}$.

correlation function of the dynamic component. The contrast value can be calculated by substituting eq. (2) into eq. (1):

$$K^2 = \frac{2\beta}{T}\int_0^T \left[(1-\rho)\left|g_{1d}(\tau)\right|+\rho\right]^2 (1-\tau/T)\,d\tau = \left[(1-\rho)^2 K_{2\,d}^2 + 2\rho(1-\rho)K_{1\,d}^2 + \beta\rho^2\right], \quad (3)$$

where $K_{2\,\mathrm{d}}^2 = 2\beta/T\int_0^T \left|g_{1\,\mathrm{d}}(\tau)\right|^2(1-\tau/T)\,d\tau$ and $K_{1\,\mathrm{d}}^2 = 2\beta/T\int_0^T \left|g_{1\,\mathrm{d}}(\tau)\right|(1-\tau/T)\,d\tau$ are the normalized variances of the intensity and field fluctuations of the dynamic part of the detected signal with $K_{2\,\mathrm{d}} < K_{1\,\mathrm{d}}$.

A correct analysis of the laser speckle image can only be performed if the value of ρ is known.[16] This can be achieved by an additional processing step . The camera exposure time T is usually larger compared to the relaxation time τ_0 related to blood flow and subsequent frames are separated by a period Δt larger or equal T. Since $\Delta t \geq T > \tau_0$ two sequential frames are free of the dynamic component of interest and thus the space dependent static component can be easily found by cross-correlating a sub-set of N pixels i, j around a given position: $\beta\rho^2 + 1 = \langle I_0 I_{\Delta t}\rangle_N / \langle I\rangle_N^2$

Fig. 3 shows results of the contrast inversion applied to our experiments. While the correct procedure yields values close to the relaxation time of Brownian motion τ_0 the direct conversion, neglecting static scattering, can deviate by several orders of magnitude.

In conclusion, we studied the image blurring of an object buried in a turbid medium and found that the resolution of the obtained images can be affected significantly by multiple scattering. We furthermore introduced a model that reflects the impact of the static scattering on the interpretation of LSI images. A simple procedure has been suggested to perform a quantitative analysis in actual LSI experiments.

Financial support from the Swiss National Science foundation (Project No. 111824) is gratefully acknowledged. Correspondence should be addressed to Frank Scheffold (e-mail, Frank.Scheffold@unifr.ch) or Pavel Zakharov (e-mail, Pavel.Zakharov@unifr.ch)

References

1. J. D. Briers. Laser doppler, speckle and related techniques for blood perfusion mapping and imaging. *Physiological Measurement*, 22(4):R35–R66, 2001.
2. B. Weber, C. Burger, M. T. Wyss, G. K. von Schulthess, F. Scheffold, and A. Buck. Optical imaging of the spatiotemporal dynamics of cerebral blood flow and oxidative metabolism in the rat barrel cortex. *Eur J Neurosci*, 20(10):2664, 2004.
3. T. Durduran, M. G. Burnett, C. Zhou G. Yu, D. Furuya, A. G. Yodh, J. A. Detre, and J. H. Greenberg. Spatiotemporal quantification of cerebral blood flow during functional activation in rat somatosensory cortex using laser-speckle flowmetry. *Journal of Cerebral Blood Flow & Metabolism*, 24:518–525, 2004.
4. A. Dunn, A. Devor, M. Andermann, H. Bolay, M. Moskowitz, A. Dale, and D. Boas. Simultaneous imaging of total cerebral hemoglobin concentration, oxygenation and blood flow during functional activation. *Optics Letters*, 28:28 – 30, 2003.
5. A.C. Völker, P. Zakharov, B. Weber, F. Buck, and F. Scheffold. Laser speckle imaging with active noise reduction scheme. *Opt. Exp.*, 13(24):9782 – 9787, 2005.
6. B.J. Berne and R. Pecora. *Dynamic Light Scattering. With Applications to Chemistry, Biology, and Physics.* Dover Publications, Inc., New York, 2000.
7. D.J. Durian. Accuracy of diffusing-wave spectroscopy theories. *Phys. Rev. E* , 51:3350 – 3358, 1995.
8. Brackets $\langle\rangle$ denote the ensemble average. In practice this average can be obtained by a spatial or temporal analysis of the intensity fluctuations, for details see Refs. 1–5
9. S. A. Prahl, M. Keijzer, S. L. Jacques, and A. J. Welch. A monte carlo model of light propagation in tissue. In G. J. Müller and D. H. Sliney, editors, *SPIE Proceedings of Dosimetry of Laser Radiation in Medicine and Biology*, volume IS 5, pages 102 – 111, 1989.
10. D. A. Zimnyakov. On some manifestations of similarity in multiple scattering of coherent light. *Waves Random Media*, 10:417 – 434, 2000.
11. D. A. Boas and A. G. Yodh. Spatially varying dynamical properties of turbid media probed with diffusing temporal light correlation. *JOSA*, 14(1):192 – 215, 1997.
12. K Schätzel. Noise on photon correlation data. i. autocorrelation functions. *Quantum Optics: Journal of the European Optical Society Part B*, 2(4):287–305, 1990.
13. R. Bandyopadhyay, A.S. Gittings, S.S. Suh, P.K. Dixon, and D.J. Durian. Speckle-visibility spectroscopy: A tool to study time-varying dynamics. *Rev. Sci. Instrum.*, 76:093110, 2005.
14. M. Heckmeier and G. Maret Visualization of Flow in Multiple Scattering Liquids, *Europhys. Lett.* 34, 257 (1996)

15. Haiying Cheng, Qingming Luo, Qian Liu, Qiang Lu, Hui Gong, and Shaoqun Zeng. Laser speckle imaging of blood flow in microcirculation. *Physics in Medicine and Biology*, 49(7):1347–1357, 2004.
16. We note that our results are in contradiction to previous claims that simply analyzing dynamic speckles eliminates the *contamination* due to stationary speckles as reported by P. Li, S. Ni, L. Zhang, S. Zeng, and Q . Luo Imaging cerebral blood flow through the intact rat skull with temporal laser speckle imaging. *Optics Letters*, 31:1824 – 1827, 2006.